The Effect of Relative Humidity on Binary Gas Diffusion

Nelson G. C. Astrath,* Jun Shen,* Datong Song, Jurandir H. Rohling, Francine B. G. Astrath, Jianqin Zhou, Titichai Navessin, Zhong Sheng (Simon) Liu, Caikang E. Gu, and Xinsheng Zhao

National Research Council of Canada, Institute for Fuel Cell Innovation, 4250 Wesbrook Mall, Vancouver, British Columbia V6T 1W5 Canada

Received: January 27, 2009; Revised Manuscript Received: February 20, 2009

The dependence of diffusion coefficient of O_2-N_2 mixture in the presence of water vapor was experimentally determined as a function of relative humidity (RH) with different temperatures using an in-house made Loschmidt diffusion cell. The experimental results showed that O_2-N_2 diffusion coefficient increased more than 17% when RH increased from 0% to 80% at 79 °C. In the experiments, the RH in both top and bottom chambers of the diffusion cell were the same, and the pressure inside the diffusion cell was kept as ambient pressure (1 atm.). Maxwell-Stefan theory was employed to analyze the mass transport in the diffusion cell, and found that there was no effective water vapor diffusion taking place, indicating that the gas diffusion in this ternary (O_2-N_2-water vapor) system could be considered binary gas (O_2-N_2) diffusion. The Fuller, Schettler, and Giddings (FSG) empirical equation of the kinetic theory of gases was generalized to accommodate the dependence of the binary diffusion coefficient on the RH. The prediction of the generalized equation was found to be consistent with experimental results with the difference of less than 1.5%, showing that the generalized equation could be applied to calculate the diffusion coefficients of the binary gaseous mixture with different temperature and RH values. The effect of water vapor on the increase of O_2-N_2 diffusion coefficient was discussed using molecule theory.

Introduction

Thanks to the well-known significance of gaseous diffusion in a wide variety of chemical processes, the temperature and pressure dependence of the diffusion coefficient (namely diffusivity) were theoretically and experimentally investigated for numerous binary gas systems.[1,2] Over a century, considerable efforts were made to develop a dependable and general equation to predict the binary gas diffusion coefficients for several binary systems. For this purpose, Arnold,[3] Gilliland,[4] Chapman and Enskog,[5] Hirschfelder, Bird and Spotz,[6] Chen and Othmer,[7] Fuller, Schettler and Giddings (FSG),[8] and Huang and coworkers[9] developed empirical equations of the kinetic theory of gases based on Stefan−Maxwell's hard sphere model. Among them FSG[8] developed a successful equation in which atomic and structural volume increments were obtained by a comparison between their theory and more than 500 measurements.[1] As indicated by Karaiskakis and Gavril, the FSG equation provides the best practical combination of simplicity and accuracy.[1] However, all of these equations cannot predict the influence of humidity on binary gas diffusion. The determination of O_2-N_2 diffusion in the presence of water vapor is relevant to numerous chemical and electrochemical reactions. For example, in a proton exchange membrane fuel cell, at variable relative humidity (RH) value oxygen is transported from an air-flow channel, through a gas diffusion layer and then into a cathode catalyst layer, where an oxygen reduction reaction takes place. The rate of diffusion of oxygen affects significantly the power output of the proton exchange membrane fuel cell. In this context, the knowledge of the binary gas diffusion coefficient in different gas humidity is crucial for the development of an accurate theoretical prediction and simulation of fuel cell performance.[10]

In this work the influence of humidity on binary gas (O_2-N_2) diffusion was theoretically and experimentally examined. Maxwell−Stefan theory was employed to study the O_2-N_2 diffusion in the presence of water vapor as a ternary system, and the numerical simulation showed that under a certain condition the diffusion could be treated as binary gas diffusion. O_2-N_2 diffusion coefficients were measured under various experimental conditions of different temperatures and relative humidity using an in-house made gas diffusion cell. The FSG equation was generalized to accommodate the dependence of the diffusion coefficient on relative humidity. The prediction of the generalized equation was found to be well consistent with experimental data, exhibiting that the generalized equation could be used to calculate O_2-N_2 diffusion coefficients with various temperatures and relative humidity.

Experimental Section

Experimental Setup. Figure 1 shows a Loschmidt diffusion cell used in this work.[11] It consisted of the top and bottom chambers. The interior length and diameter of each chamber were $0.5L = 17.75$ and 2.06 cm, respectively. They could be connected (5a) or separated (5b) by a ball valve (5) (Apollo 86-104-49). The upper side of the ball valve marked the middle of the diffusion cell ($z = 0$), and the ball valve was part of the bottom chamber. Two mass flow controllers (Omega, model FMA-5508 0-500 mL/min) were connected to two inlets (1 and 2) to control the gas flow rate when gases were filled into the chambers. An oxygen sensor (Ocean Optics FOXY-AL300) was employed to measure gas diffusion coefficients. Its 300 μm (in diameter) aluminum jacketed optical fiber probe was installed in the top chamber at the position very close to $z = 1.9$ cm (6).

* To whom correspondence should be addressed. E-mail: Jun.Shen@nrc-cnrc.gc.ca, AstrathNGC@pq.cnpq.br.

10.1021/jp900796w CCC: $40.75 Published 2009 by the American Chemical Society
Published on Web 05/26/2009

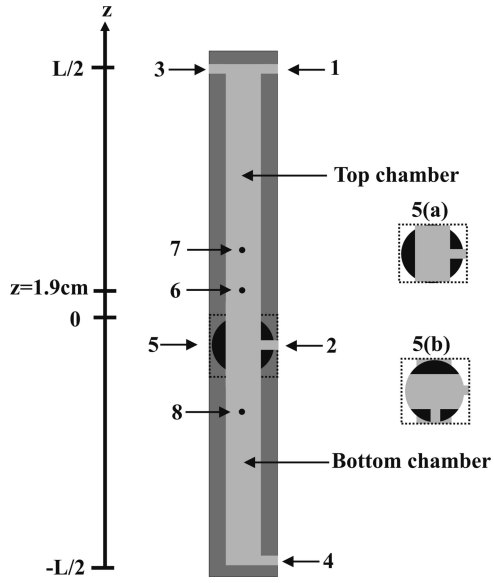

Figure 1. Schematic diagram of a diffusion cell: (1) inlet 1 for gas N_2; (2) inlet 2 for gas O_2; (3 and 4) outlets; (5) ball valve; (5a) ball valve (open); (5b) ball valve (closed); (6) oxygen sensor; (7 and 8) humidity sensors.

On the tip of the optical fiber probe was the ruthenium complex in a sol−gel substrate. The probe was connected to an excitation source and a spectrometer (Ocean Optics S2000-FL) by a bifurcated optical fiber. The spectrometer was connected by a computer via a USB A/D converter (Ocean Optics ADC 1000). According to the vender, the response time of the oxygen sensor is around 1 s and the accuracy is 1% of full range for 0−100% (mole percent).

In this work, we measured binary diffusion coefficients of O_2−N_2 with different humidity and temperature. To fill the gases into the diffusion cell, first, with the inlet 2 and outlet 3 closed and the ball valve opened (5a), both chambers (top and bottom) were filled with gas 1, N_2, through the inlet 1 for 15 min at a flow rate of 500 mL/min. Meanwhile, the outlet 4 was open to expel the originally existing gas. Second, after both inlet 1 and outlet 4 were closed, the ball valve was closed (5b). Third, the bottom chamber was filled with gas 2, O_2, through inlet 2 for 12 min at a flow rate of 500 mL/min, at the same time outlet 4 was open to drive out gas N_2. Fourth, both inlet 2 and outlet 4 were closed. Finally, both outlet 3 and outlet 4 were opened for around 15 s then were closed. In this way the pressure inside of the diffusion cell kept as the ambient pressure. The chambers, pipes and valves were temperature controlled. A humidifier (TesSol FCTS BH 500) was coupled into both gas suppliers, inlet 1 and 2, to control the relative humidity (RH) values of the gases from 0 to 90%. The RH in both chambers was monitored using two RH sensors (7 and 8) (Sensirion SHT75).

After the gases were filled into the diffusion cell, the oxygen sensor was employed to measure the O_2 concentration evolution in the top chamber. Before the diffusion started, the oxygen sensor signal was monitored for about 120 s to make sure the system was stable. This signal was also used as a baseline. When the ball valve was opened, the gas diffusion started, and the concentration of O_2 in the top chamber began to increase. The time-resolved signal from the O_2 sensor was recorded, and the whole measurement system was controlled by the computer.

Signal Processing. In the experiments the top and bottom chambers were initially filled with two gases: gas 1 (N_2, species 1) and gas 2 (O_2, species 2), respectively, with the same RH. When theses two chambers were connected at $t = 0$, the diffusion started. The O_2−N_2 diffusion in the presence of water vapor is a ternary system, and Maxwell−Stefan theory is employed to analyze gas transport in the diffusion cell. Mass fractions for two of the three components are solved, and the third one is given by the first two. The three governing equations are[12]

$$\rho\frac{\partial\omega_1}{\partial t} + \nabla\cdot\left(-\rho\omega_1\sum_{k=1}^{3}\left[\tilde{D}_{1k}\left(\nabla x_k + (x_k - \omega_k)\frac{\nabla p}{p}\right)\right] - \mathbf{D}^{\dagger}\frac{\nabla T}{T}\right) = -\rho\mathbf{u}\cdot\nabla\omega_1 \quad (1)$$

and

$$\rho\frac{\partial\omega_2}{\partial t} + \nabla\cdot\left(-\rho\omega_2\sum_{k=1}^{3}\left[\tilde{D}_{2k}\left(\nabla x_k + (x_k - \omega_k)\frac{\nabla p}{p}\right)\right] - \mathbf{D}^{\dagger}\frac{\nabla T}{T}\right) = -\rho\mathbf{u}\cdot\nabla\omega_2 \quad (2)$$

for N_2 and O_2 mass fractions, ω_1 and ω_2, respectively. Water vapor mass fraction is $\omega_3 = 1 - \omega_1 - \omega_2$.

In eqs 1 and 2 $\mathbf{D}^{\dagger}$ is the transpose of the diffusion coefficient matrix $\mathbf{D} = (D_{ik})$ ($cm^2\ s^{-1}$), and p the total pressure (Pa). T is the temperature (K), and $\mathbf{u}$ the velocity vector ($cm\ s^{-1}$); x and ω are mole fraction and mass fraction, respectively. The mixture density, ρ ($g\ cm^{-3}$), is a function of the average mixture mole fraction of the mixture mole mass, M ($g\ mol^{-1}$), and the mixture mole fractions,

$$M = \sum_i x_i M_i \quad (3)$$

and

$$\rho = \frac{p}{RT}M \quad (4)$$

Here M_i is the mole mass of component i. Note that $\tilde{D}_{ik}$ is the (i,k) component of the multicomponent Fick diffusivity matrix $\tilde{\mathbf{D}}$. It can be calculated from Maxwell−Stefan diffusivities/binary diffusivities, D_{ik}, which is given by[13]

$$pD_{\mathrm{vapor,N_2}} = 0.2599\left(\frac{T}{299.42}\right)^{2.334}$$
$$pD_{\mathrm{vapor,O_2}} = 0.3022\left(\frac{T}{323.83}\right)^{2.334}$$
$$pD_{\mathrm{O_2,N_2}} = 0.0544\left(\frac{T}{143.01}\right)^{1.823} \quad (5)$$

Here i, k = vapor, N_2, and O_2. Vapor stands for water vapor. The saturated water vapor pressure is given by[14]

$$p_{\mathrm{vapor}}^{\mathrm{sat}} = \exp\left(11.6832 - \frac{3816.44}{T - 46.13}\right) \quad (6)$$

The problem is solved by the Maxwell−Stefan diffusion and convection application mode in the Chemical Engineering Module of COMSOL Multiphysics software.[12] There is no imposed fluid velocity. The boundary conditions at the top and bottom of the cell should be insulated. The initial conditions for each species are

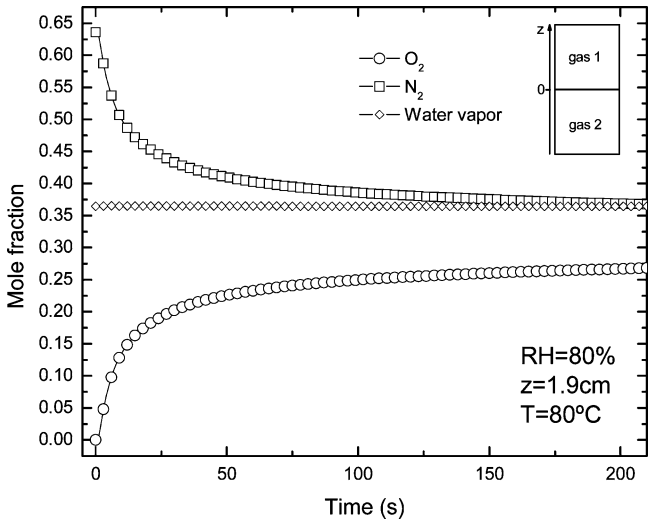

Figure 2. Concentration (mole fraction) evolution of O_2, N_2, and water vapor at $z = 1.9$ cm, RH = 80% and $T = 80$ °C, calculated using the ternary model.

$$x_{\text{vapor}}(t=0) = \frac{\text{RH}_{\text{bottom}} \times p^{\text{sat}}_{\text{vapor}}}{p}$$
$$x_{\text{N}_2}(t=0) = 0$$
$$x_{\text{O}_2}(t=0) = 1 - x_{\text{vapor}}(t=0) - x_{\text{N}_2}(t=0)$$
$$\omega_{\text{N}_2}(t=0) = (x_{\text{N}_2}(t=0) \times M_{\text{N}_2})/(x_{\text{O}_2}(t=0) \times M_{\text{O}_2} + x_{\text{N}_2}(t=0) \times M_{\text{N}_2} + x_{\text{vapor}}(t=0) \times M_{\text{vapor}})$$
$$\omega_{\text{O}_2}(t=0) = (x_{\text{O}_2}(t=0) \times M_{\text{O}_2})/(x_{\text{O}_2}(t=0) \times M_{\text{O}_2} + x_{\text{N}_2}(t=0) \times M_{\text{N}_2} + x_{\text{vapor}}(t=0) \times M_{\text{vapor}})$$
$$\omega_{\text{vapor}}(t=0) = 1 - \omega_{\text{O}_2}(t=0) - \omega_{\text{N}_2}(t=0) \quad (7)$$

for the bottom chamber and

$$x_{\text{vapor}}(t=0) = \frac{\text{RH}_{\text{top}} \times p^{\text{sat}}_{\text{vapor}}}{p}$$
$$x_{\text{O}_2}(t=0) = 0$$
$$x_{\text{N}_2}(t=0) = 1 - x_{\text{vapor}}(t=0) - x_{\text{O}_2}(t=0)$$
$$\omega_{\text{N}_2}(t=0) = (x_{\text{N}_2}(t=0) \times M_{\text{N}_2})/(x_{\text{O}_2}(t=0) \times M_{\text{O}_2} + x_{\text{N}_2}(t=0) \times M_{\text{N}_2} + x_{\text{vapor}}(t=0) \times M_{\text{vapor}})$$
$$\omega_{\text{O}_2}(t=0) = (x_{\text{O}_2}(t=0) \times M_{\text{O}_2})/(x_{\text{O}_2}(t=0) \times M_{\text{O}_2} + x_{\text{N}_2}(t=0) \times M_{\text{N}_2} + x_{\text{vapor}}(t=0) \times M_{\text{vapor}})$$
$$\omega_{\text{vapor}}(t=0) = 1 - \omega_{\text{O}_2}(t=0) - \omega_{\text{N}_2}(t=0) \quad (8)$$

for the top chamber. With the initial conditions that the RH is the same in both chambers (e.g., RH = 80%), and the top and bottom chamber fills with nitrogen and oxygen, respectively, the simulation results are given in Figures 2−4. Both transient and steady analysis (Figures 2 and 3) show that the mole fraction of water vapor in the diffusion cell is a constant while oxygen diffuses from the bottom chamber to the top chamber, and nitrogen diffuses from the top chamber to the bottom one. For the transient behavior of O_2 mole fraction under different RH values at $z = 1.9$ cm, Figure 4 shows a significant drop in the case of RH = 80%, compared to the case of RH = 0%.

The numerical simulation shown in Figures 2 and 3, in which concentration of water vapor keeps a constant in the ternary system, suggests that with the aforementioned initial conditions there is no effective water vapor diffusion taking place, and

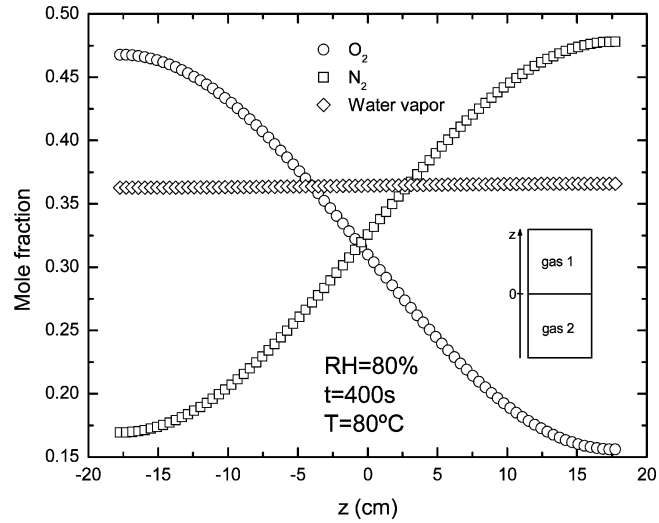

Figure 3. Concentration (mole fraction) distribution of O_2, N_2, and water vapor at $t = 400$ s, RH = 80% and $T = 80$ °C, calculated using the ternary model.

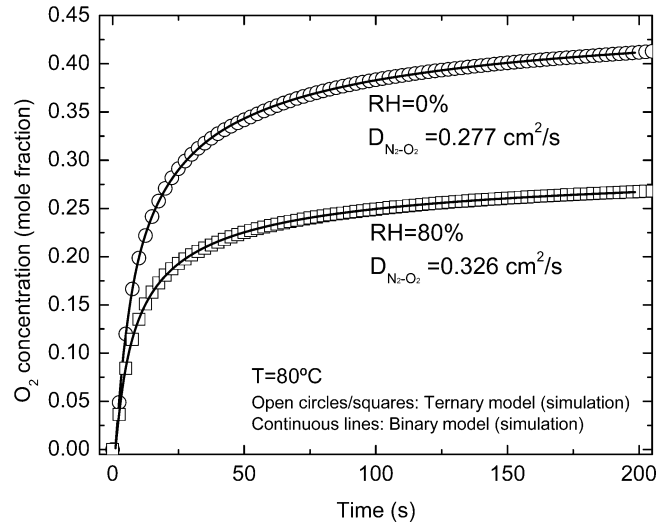

Figure 4. Concentration (mole fraction) evolution of O_2 at z= 1.9 cm for RH = 0% and RH = 80% at $T = 80$ °C, calculated using both the ternary model and binary model.

the gas diffusion in this ternary system might be considered binary gas (O_2−N_2) diffusion. When the diffusion coefficient D_{21} is a constant, Fick's second law of diffusion describes the one-dimensional binary diffusion as[15]

$$\frac{\partial \eta_2}{\partial t} = D_{21} \frac{\partial^2 \eta_2}{\partial z^2} \quad (9)$$

Here η_2 stands for the concentration of species (gas) 2. One can solve eq 9 with the following initial and boundary conditions:

$$\eta_2 = \eta_2^{\text{b}} \qquad (-L/2 \le z < 0,\ t = 0)$$
$$\eta_2 = \eta_2^{\text{t}} \qquad (0 < z \le +L/2,\ t = 0)$$
$$\left(\frac{\partial \eta_2}{\partial z}\right)_{z=\pm L/2} = 0 \qquad (t > 0) \quad (10)$$

The last equation of the initial and boundary conditions is the impermeable boundary conditions at $z = \pm L/2$, which means zero flow across the boundaries.[15] The η_2^{b} and η_2^{t} are the concentrations of gas 2 at $t = 0$ in bottom and top chambers,

respectively. In this work the η_2^t is zero. The solution can be expressed as[11]

$$\eta_2(z,t) = \frac{1}{2}(\eta_2^b + \eta_2^t) - \frac{2(\eta_2^b - \eta_2^t)}{\pi}\sum_{m=0}^{\infty}\frac{\exp(-(2m+1)^2\pi t/\tau)}{(2m+1)}\sin\left[\frac{(2m+1)\pi z}{L}\right] \quad (11)$$

τ is the characteristic diffusion time defined as

$$\tau = \frac{L^2}{\pi D_{21}} \quad (12)$$

L in eqs 11 and 12 is the length of the Loschmidt cell shown in Figure 1. The τ can be found by fitting the theoretical model to experimental data or be calculated with the knowledge of D_{21}. At 25 °C $D_{21} = 0.202$ cm$^2 s^{-1}$ for dry O_2-N_2 diffusion;[16] with the dimension of this experimental diffusion cell the τ is about 2000 s.

Equation 11 is a general solution and converges most satisfactorily for large values of time.[15] In practice, sometimes the measurement for short-time diffusion is convenient and required. For an infinite space and with the initial distribution of gas 2

$$\eta_2 = \eta_2^b \qquad z < 0, \quad t = 0$$
$$\eta_2 = 0 \qquad z > 0, \quad t = 0 \quad (13)$$

the solution of eq 19 can be found in ref 15

$$\eta_2(z,t) = \frac{1}{2}\eta_2^b \,\mathrm{erfc}\left(\frac{z}{2\sqrt{D_{21}t}}\right) \quad (14)$$

in which erfc(x) is the complementary error function. Equation 14 is suitable for numerical evaluation at small time,[15] during which the diffusion occurs in a finite region.

In the case that the initial condition $\eta_2 = \eta_2^t$ ($z > 0$, $t = 0$), eq 14 can be rewritten as

$$\eta_2(z,t) = \frac{1}{2}\left[\eta_2^b + \eta_2^t - (\eta_2^b - \eta_2^t)\,\mathrm{erf}\left(\frac{z}{2\sqrt{D_{21}t}}\right)\right] \quad (15)$$

erf(x) is the error function. Reference 11 shows that when $t < 0.1\ \tau$, 90% of the diffusion gases have not reached to the impermeable boundaries, and the difference between the infinite space approximation and the general solution is less than 1%. Therefore this approximation can be used to describe the binary diffusion when the diffusion duration is less than 0.1 τ.[11]

Figure 4 shows the comparison of oxygen concentration evolution in the top chamber simulated by ternary transportation model and binary diffusion model for 0 and 80% RH, respectively. The diffusivities used for the simulations are shown in the figure. The largest difference between the two simulations is less than 1%. This consistency indicates that the O_2-N_2 diffusion in the presence of water vapor can be considered binary diffusion, probably due to no effective diffusion of water vapor occurring under the foregoing experimental conditions. It can be concluded that the binary diffusion model can be employed for signal processing.

Experimental results have proven the conclusion. Figure 5 shows a typical concentration evolution pattern of the gas diffusion measured using the oxygen sensor for the binary gas mixture O_2-N_2 at 79 °C under the conditions of RH = 0% and RH = 80%, respectively. The continuous lines in Figure 5 represent the least-squares curve fitting of eq 15 to the experimental data. In the experiments, the exact time t_0 of the beginning of the gas diffusion was unknown. To find t_0, the t in eq 15 was replaced by $t - t_0$ when curve fittings were performed. The values of the diffusion coefficient was found to be $D_{21} = (0.278 \pm 0.003)$ cm^2 s^{-1} at 79 °C with RH = 0%, which is consistent with the literature value $D_{21} = 0.277$ cm^2 s^{-1} at 80 °C with RH = 0%,[16] exhibiting that the binary diffusion model is suitable for the signal processing. Also, $D_{21} = (0.326 \pm 0.005)$ cm^2 s^{-1} at 79 °C in the presence of RH = 80% was determined. The fact that standard deviation was less than 1.6% demonstrated that precise experimental results could be achieved with the experimental setup and signal process method described in this "Experimental" section.

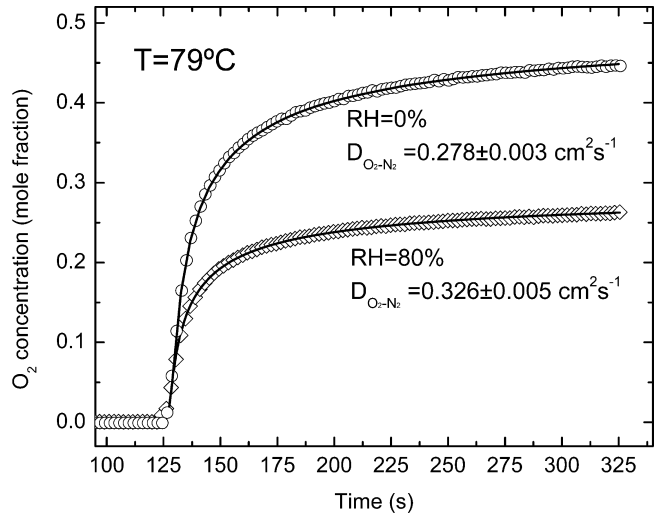

Figure 5. The concentration evolution of O_2 in a binary gas mixture of O_2-N_2 at 79 °C measured by oxygen sensor (RH = 0%, open circles; RH = 80%, open squares). The continuous lines represent the best curve fittings using eq 15 to the experimental data.

Results and Discussion

O_2-N_2 Diffusion under Dry Condition. The measured temperature dependency of O_2-N_2 diffusion coefficient under dry condition is shown in Figure 6. The diffusion coefficient at 25 °C is in good agreement with the literature value (0.202 cm^2 s^{-1}),[16] and the measured temperature dependence of the diffusion coefficient is consistent with that calculated using the FSG equation:

$$D_{21} = \frac{1.00 \times 10^{-3} T^{1.75}(1/M_1 + 1/M_2)^{1/2}}{p[(\sum v)_1^{1/3} + (\sum v)_2^{1/3}]^2} \quad (16)$$

The diffusion coefficient of an ideal binary system 1−2 (D_{21}) is a function of temperature, pressure, and concentration.[17] The empirical correlation, eq 16, successfully developed by Fuller, Schettler, and Giddings (FSG) permits the evaluation of the diffusivity for gas pairs of nonpolar and nonreacting molecules based on the special atomic diffusion volumes.[8,18] This equation is more accurate in predicting D_{21} compared to other empirical models.[1] In the equation, D_{21} is the mass diffusivity of gas 2 through gas 1; T is the absolute temperature, K; p is the absolute pressure, atm, with the atomic and structural diffusion volume increment[8,18] v to be summed over the atoms, group of atoms, and structural features of each diffusion species. The vs values were determined from a nonlinear least-squares analysis of over 500 experimental points and are given for some simple

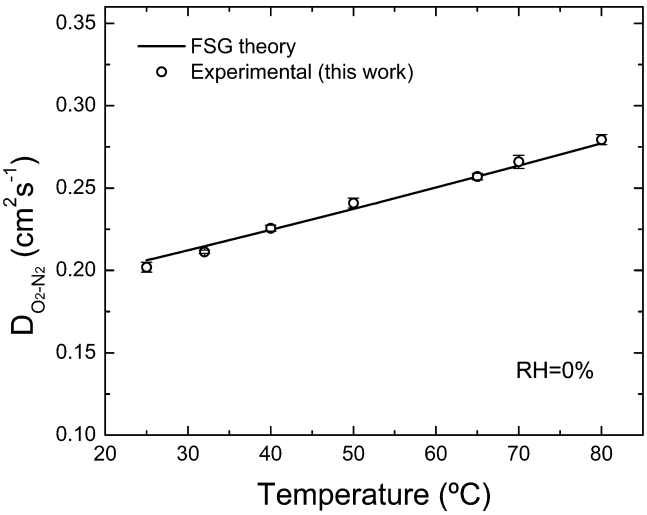

Figure 6. Temperature dependence (25−79 °C) of the diffusion coefficient of binary gas mixture of N_2-O_2 under dry condition measured using the oxygen sensor (open circles): Open circles, experimental data; solid line, the theoretical prediction using the FSG equation, eq 7. The following parameters were used in the theoretical calculations:[17] $(\sum v)_{N_2} = 18.5$; $(\sum v)_{O_2} = 16.3$; $p = 1$ atm; $M_{N_2} = 28$ g/mol and $M_{O_2} = 32$ g/mol.

molecules elsewhere.[18] M_1 and M_2 are the molecular masses of gas 1 and gas 2, respectively, g/mol. Our experimental results, once again, demonstrate the reliability of the FSG equation in the calculation of diffusion coefficients of a dry binary gas mixture.

O_2-N_2 Diffusion in the Presence of Water Vapor. The FSG theory can predict the temperature and pressure dependence of diffusion coefficients of a dry binary mixture, but it is not suitable for the binary system in the presence of humidity. To study the influence of the humidity, we performed diffusion measurements at two different temperatures, 69 and 79 °C, varying the relative humidity from 0 to 80% for each temperature. As mentioned in the experimental section, a humidifier system was used to control the RH of both gases, which were filled into the diffusion chambers with the same RH. The measured results of $D_{21} = D_{O_2-N_2}$ are shown in Figure 7. At the temperature of 79 °C, the diffusion coefficient varies from (0.278 ± 0.003) under a dry condition to (0.326 ± 0.005) cm^2 s^{-1} with 80% RH; the $D_{O_2-N_2}$ changes from (0.265 ± 0.003) to (0.262 ± 0.002) cm^2 s^{-1} at 69 °C. To our best knowledge, this is the first time that the diffusion coefficient of binary gas mixtures is measured as a function of relative humidity.

In the experiments, the top and bottom chambers had the same volume V, and the pressure in the diffusion cell was kept as the ambient pressure. At $t = 0$ the total pressure in the bottom (P_{BOT}) and top (P_{TOP}) chambers could be written, respectively, as

$$P_{TOP} = P_{N_2} + P_{vapor} = (n_{N_2}^{RH} + n_{vapor}^{RH})RT/V = \left(\frac{\rho_{N_2}^{RH}}{M_{N_2}} + \frac{\rho_{vapor}^{RH}}{M_{H_2O}}\right)RT$$

$$P_{BOT} = P_{O_2} + P_{vapor} = (n_{O_2}^{RH} + n_{vapor}^{RH})RT/V = \left(\frac{\rho_{O_2}^{RH}}{M_{O_2}} + \frac{\rho_{vapor}^{RH}}{M_{H_2O}}\right)RT \quad (17)$$

P_i,n_i^{RH}, and ρ_i^{RH} are the partial pressure, number of moles, and mass density of the gas i at the relative humidity. T is temperature in K, and R is the universal gas constant. Compared with the experiments with dry gases (i.e., RH = 0%), the presence of water vapor (RH ≠ 0) reduces the partial pressure

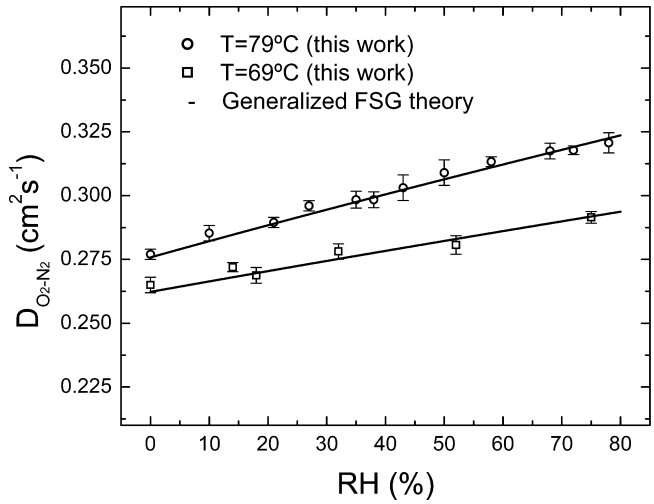

Figure 7. Humidity dependence of the diffusion coefficient of a binary gas mixture of O_2-N_2 at 69 °C (open squares) and at 79 °C (open circles) measured using the oxygen sensor. The continuous lines represent the theoretical prediction using the generalized FSG theory, eq 22. The following parameters were used in the theoretical calculations: $(\sum v)_{H_2O} = 13.1$ and $M_{H_2O} = 18$ g/mol.

or the mass density (concentration) of the diffusion gases (e.g., N_2 and O_2). The mole fraction η_i^{RH} of diffusion gas i in the presence of water vapor (measured by RH) can be expressed as a mole fraction

$$\eta_i^{RH} = \frac{n_i^{RH}}{n_i^{RH} + n_{vapor}^{RH}} \quad (18)$$

with

$$n_i^{RH} = \frac{\rho_i^{RH} V}{M_i} n_{vapor}^{RH} = \frac{\rho_{vapor}^{RH} V}{M_{H_2O}} \quad (19)$$

Here $\rho_{vapor}^{RH} = 100\rho_{sat}$RH (RH is in percentage), and ρ_{sat} is the saturation vapor density that can be calculated using the saturation vapor pressure.[19] Knowing the RH value, ρ_i^{RH} can be calculated using eq 17, and then η_i^{RH} can be obtained with the equations above. In comparison with the dry binary gas mixture, the presence of water vapor reduces the concentration and therefore the mass M_i^{RH} of gas i in one mole of the mixture of gas i and water vapor in a chamber at $t = 0$, that is

$$M_i^{RH} = \eta_i^{RH} M_i \quad (20)$$

During the diffusion processes with water vapor, the self-diffusion of the water vapor between the chambers does not play an important role. On the other hand, the water vapor inside the chambers is working as molecular barriers, contributing to the diffusion volume v. Thus, the sum of all diffusion volume portions is

$$(\sum v)_i^{RH} = \eta_i^{RH} v_i + \eta_{H_2O}^{RH} v_{H_2O} \quad (21)$$

Substituting eqs 20 and 21 into FSG eq 16, one can express the diffusion coefficient for different RH values as

$$D_{21}^{RH} = \frac{1.00 \times 10^{-3} T^{1.75} \left(\frac{1}{\eta_1^{RH} M_1} + \frac{1}{\eta_2^{RH} M_2}\right)^{1/2}}{p[(\eta_1^{RH} v_1 + \eta_{H_2O}^{RH} v_{H_2O})^{1/3} + (\eta_2^{RH} v_2 + \eta_{H_2O}^{RH} v_{H_2O})^{1/3}]^2} \quad (22)$$

The solid lines in Figure 7 represent the theoretical calculation using eq 22. The parameters used to calculate the diffusion

coefficient for different RH are listed in the figure captions of Figures 6 and 7. Comparing the measured diffusion coefficients with the calculated ones, the relative error at different humidity and temperature was less than 1.5%, showing a good agreement between the generalized FSG equation and experimental data. When RH = 0%, that is, dry gases, eq 22 returns to the FSG eq 16, and therefore eq 22 is a generalized version of the FSG equation.

Mass diffusion coefficient can be expressed in terms of the product of the mean thermal speed (υ) and the mean free path (λ) as $D \propto \upsilon\lambda$. It is known that the mean thermal speed is proportional to the temperature and inversely proportional to the molar mass[17] of the gas mixture. Compared to the dry gas mixture (e.g., N_2 and O_2), the presence of water vapor reduces the molar mass of the gas mixture and, therefore, increases the mean thermal speed. The mean free path is inversely proportional to the product of the number of molecules per unit volume and the effective cross section area for collision in the gas mixture. The presence of water vapor molecules reduces the effective cross section, which is evident considering water vapor has smaller diffusion volume compared with that of the diffuse gases, and then increases the mean free path. The molecular barriers created by the vapor induce less resistance to the mass transport, and the behavior of the diffusion coefficient with the water vapor content measured by RH is governed by the increasing of the mean thermal speed υ and mean free path λ.

Conclusions

The O_2-N_2 diffusion in the presence of water vapor has been theoretically and experimentally investigated. Under the experimental conditions, the ternary (O_2-N_2-water vapor) system has been studied using Maxwell−Stefan equation, showing that there is no effective vapor diffusion in the diffusion cell, and the O_2-N_2 diffusion in the presence of water vapor can be considered binary diffusion. A generalized FSG equation has been developed and found to be consistent with experimental data changing with temperature and RH, exhibiting that the generalized FSG equation can be applied to predict the diffusion coefficient of O_2-N_2 binary system in the presence of water vapor. The increase of O_2-N_2 diffusion coefficient in the presence of water vapor is due to the increase of the mean thermal speed and mean free path introduced by the water vapor.

References and Notes

(1) Karaiskakis, G.; Gavril, D. *J. Chromatogr., A* **2004**, *1037*, 147.
(2) Massman, W. J. *Atmos. Environ.* **1998**, *32*, 1111.
(3) Arnold, J. H. *J. Am. Chem. Soc.* **1930**, *22*, 1091.
(4) Gilliland, E. R. *Ind. Eng. Chem.* **1934**, *26*, 681.
(5) Chapman, S.; Cowling, T. G. *The Mathematical Theory of Non-Uniform Gases*; Cambridge University Press: London, 1952.
(6) Hirschfelder, J. O.; Curtiss, C. F.; Bird, R. B. *Molecular Theory of Gases and Liquids,* 2nd ed.; Wiley: New York, 1954.
(7) Chenp, N. H.; Othmer, D. P. *J. Chem. Eng. Data* **1962**, *7*, 37.
(8) Fuller, E. N.; Schettler, P. D.; Giddings, J. C. *Ind. Eng. Chem.* **1966**, *58*, 19.
(9) Huang, T.-C.; Young, F. J. F.; Huang, C.-J.; Kuo, C.-H. *J. Chromatogr.* **1972**, *70*, 13.
(10) Wang, Q.; Eikerling, M; Song, D; Liu, Z.; Navessin, T.; Xie, Z; Holdcroft, S. *J. Electrochem. Soc.* **2004**, *151*, A950.
(11) Rohling, J. R.; Shen, J.; Wang, C.; Zhou, J.; Gu, C. E. *Appl. Phys. B: Laser Opt.* **2007**, *87*, 355.
(12) COMSOL Multiphysics, Chemical Engineering Module, User's Guide; COMSOL AB, 2005.
(13) Bird, R. B.; Stewart, W. E.; Lightfoot; E. N. *Transport Phenomena,* 2nd ed.; John Wiley & Sons Inc.: New York, 2002.
(14) Incropera, F. P.; Dewitt, D. P.; *Fundamentals of Heat and Mass Transfer,* 3rd ed.; John Wiley & Sons, Inc.: New York, 1990.
(15) Crank, J. *The Mathematics of Diffusion,* 2nd ed.; Oxford University Press: New York, 1975.
(16) Marrero, T. R.; Mason, E. A. J. *Phys. Chem. Ref. Data* **1972**, *1*, 3.
(17) Poling, B. E.; Prausnitz, J. M.; O'Connell. J. P. *The Properties of Gases and Liquids,* 5th ed.; MacGraw-Hill: New York, 2000.
(18) Fuller, E. N.; Ensley, K.; Giddings, J. C. *J. Phys. Chem.* **1969**, *73*, 3679.
(19) Lide, D. R. *CRC Handbook of Chemistry and Physics*, 88th ed.; CRC Press:Cleveland, OH, 1977.

JP900796W